

Weak Support Material Techniques For Alternative Additive Manufacturing Materials

Eric Barnett*, Clément Gosselin

*Département de génie mécanique, Université Laval
Québec, QC, Canada, G1V 0A6
Email: eric.barnett.1@ulaval.ca, gosselin@gmc.ulaval.ca*

Abstract

Proper support geometry design is critical for additive manufacturing (AM) techniques to be successful, particularly for material deposition AM techniques, such as fused deposition modeling (FDM). Many methods have been proposed for support geometry generation, mostly geared toward FDM and most often with the objective of minimizing support-material use and part-construction time. Here, two new support geometry algorithms are proposed, which are particularly suitable for weak support materials: the shell technique, whereby the primary support material would collapse under its own weight and thus a second support material is used to create a containment shell; the film technique, whereby a second support material is deposited as a thin film between the part and the primary support material. The proposed techniques also facilitate support material removal, a laborious manual step for many AM processes. Both techniques are demonstrated through the construction of parts using an experimental large-scale 3D foam printer.

Keywords: weak support techniques, Boolean operations, path offsetting, large-scale 3D printing;

1. Introduction

Many approaches have been proposed for physically supporting the part material during additive manufacturing (AM) processes. When typical support techniques are used, the range of candidate materials for the design of a new AM system is typically limited by the precise material control needed to print the desired part geometry. As a result, most AM materials require a relatively intensive production process, and even with the economies of scale, these materials will always be much more expensive than more readily available materials such as water, concrete, and foam. Inexpensive, recyclable, and/or reusable materials, which might otherwise seem unsuitable, become feasible options for the design of new AM systems when the support techniques introduced in this paper are used. These considerations are particularly apparent in the design of large-scale AM systems, where materials are selected primarily for their cost, and not for their idealized 3D printing characteristics [1, 2, 3, 4].

A frequently used approach to the AM support problem involves selectively fusing a liquid or semi-solid substance layer-by-layer. In selective laser sintering (SLS) [5], a laser is used to selectively bind a layer of powder; after each layer is complete, a new layer of powder is swept over the top of the previous layer. In stereolithography (SLA) [6], a substrate is lowered layer by layer into a vat of photopolymer liquid. At each layer, the photopolymer is selectively exposed to light, causing it to harden in the regions that define the part. Another approach to the problem is to separately deposit both the part and support materials, the most common example being fused deposition modeling (FDM) [7]. Often, this is called an extrusion-based approach, though material-spray AM techniques are also similar, hence the more general category is referred to as the material-deposition additive manufacturing (MDAM) approach.

For MDAM, a basic support technique can be defined as that which fills the free space encountered when a part is projected downward in its build orientation. Several implementations of this technique have been proposed [8, 9, 10, 11]. While this technique is relatively simple to define mathematically, it is inefficient for support materials that can *cantilever* to a certain extent. Many *sparse* support generation techniques have therefore been proposed to reduce both material cost and printing time [12, 13, 14]. These techniques work well for FDM because the filament being deposited is *semi-rigid*, and rapidly hardens to its final rigid state. However, many potential materials for

*Corresponding author

Abbreviations

AM additive manufacturing
FDM fused deposition modeling
MDAM material-deposition additive manufacturing

AM do not behave this way. For example, certain materials can be deposited in a soft state, and then take seconds, minutes, or even hours to harden into their final state. For example, Buswell et al. developed a concrete extrusion printing system [1], and the authors have developed 3D ice and foam printers [4, 15]. All of these materials support minimal cantilevering before significant material deformation occurs after deposition, such that the sparse support techniques listed above are not very useful. However, these materials are all relatively inexpensive, and the support materials for some of these systems are *reusable*. For these reasons, minimizing part and support material use is not nearly as important as it is for FDM.

It might be argued that these types of materials should immediately be rejected as candidates for AM, since they are inherently difficult to control, and significant part error will often accumulate after hundreds or thousands of layers of material have been deposited. This problem is addressed through geometric feedback, whereby part errors are measured periodically during construction, and corrected through modification of deposition control parameters for subsequent layers [16].

For soft AM materials, a more complete support technique is needed. In some cases, the basic method of simply filling the space underneath downward-facing areas provides insufficient support. For example, the part might need *side* support in addition to support *underneath*. Rodgers introduced an extrusion-based AM process in which different polymer materials are used, with the support material partially or totally encapsulating the 3D part [17]. In 3D ice printing, water is deposited inside a freezing environment but does not freeze instantly and surface tension is relied on to prevent the water from spreading, when the basic support method is used [15]. To increase the maximum layer thickness, the basic support technique was modified to include *side* support of the deposited water, essentially providing an ascending mold for the water.

In this paper, the *shell* and *film* support techniques are introduced, which are most suitable for weak or soft support materials, such as gels or foams. These materials are assumed to *stay* soft, i.e., their material strength is weak following deposition and does not strengthen with time, or might even degrade. Such materials can be desirable for reasons of cost, material compatibility with the part, and/or ease of support removal. For the shell technique, the soft material occupies all the space specified with the basic method, and is contained by a rigid shell, composed of a second support material, which could potentially be the part material itself. Additional space is created between the shell and the part to prevent them from touching, and this space is also filled with the soft support. The film technique, transforms the basic technique to create a thin film between the part and the primary rigid support. The film should weakly bond with the part material to facilitate support removal, and can be a soft material, such as that described for the shell technique. The idea to use a second support material as a film was described in

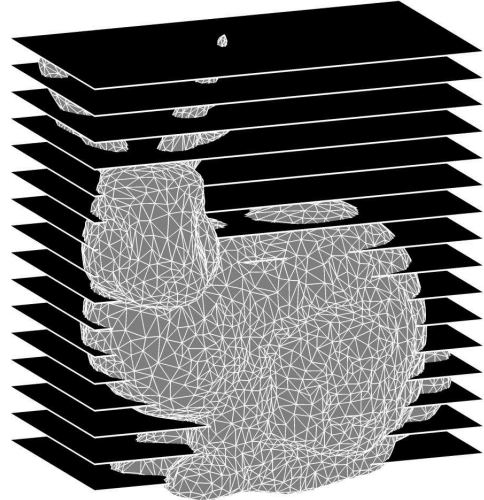


Figure 1: The Stanford bunny, with 15 slicing planes partially shown.

[18, 19], though no algorithms were reported there to implement the technique. Here, the shell and film techniques are disclosed as algorithms, which consist of a series of Boolean operations and path offsetting steps, applicable to layer data produced by slicing a part with a general 3D geometry.

Both techniques are applied to build parts using a large-scale 3D foam printer. The applicability of both support techniques is described, along with a method for adapting the film technique to support a wider variety of 3D part geometries. Then, the computational performance of all three support techniques is compared. Finally, specific areas where additional research can be conducted are identified, including the generalization of an open fill path technique for AM slice areas.

2. Weak Support Techniques

In this section a basic support technique using set operations is first described. Then, two alternative techniques for weak support materials, called the shell technique and the film technique, are introduced. All three methods are applied to the Stanford bunny [20], sliced at the 15 layers shown in Fig. 1. A 2D schematic illustrating the three techniques is shown in Fig. 2. Figure 3 shows 3D plots of the material slice areas generated when each method is applied to the Stanford bunny, for the 15 layers shown in Fig. 1.

2.1. Basic Technique

For the basic support technique, support material occupies all space encountered when a part is projected downward. Initially, the part is intersected with n equidistant horizontal planes, dividing it into n layers, as shown in Fig. 1. Therefore, a part-defining planar region or slice area P_i is formed for each layer i , delimited by external and internal contours. The series of boolean operations

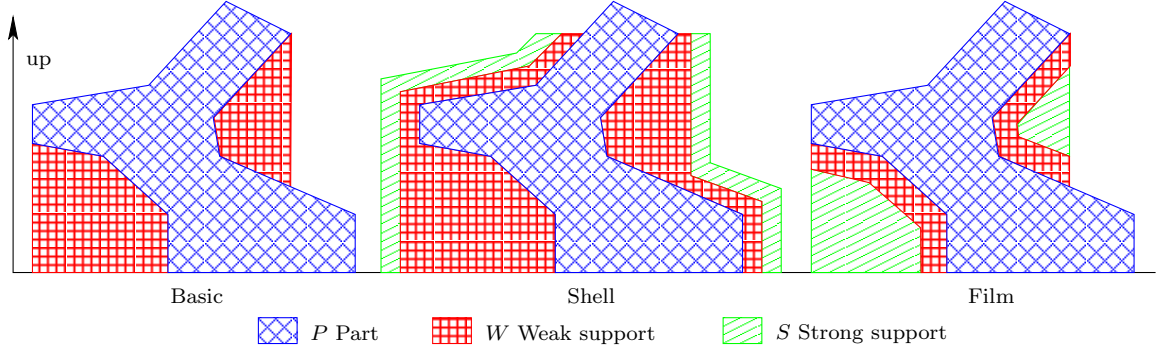


Figure 2: Additive manufacturing support techniques.

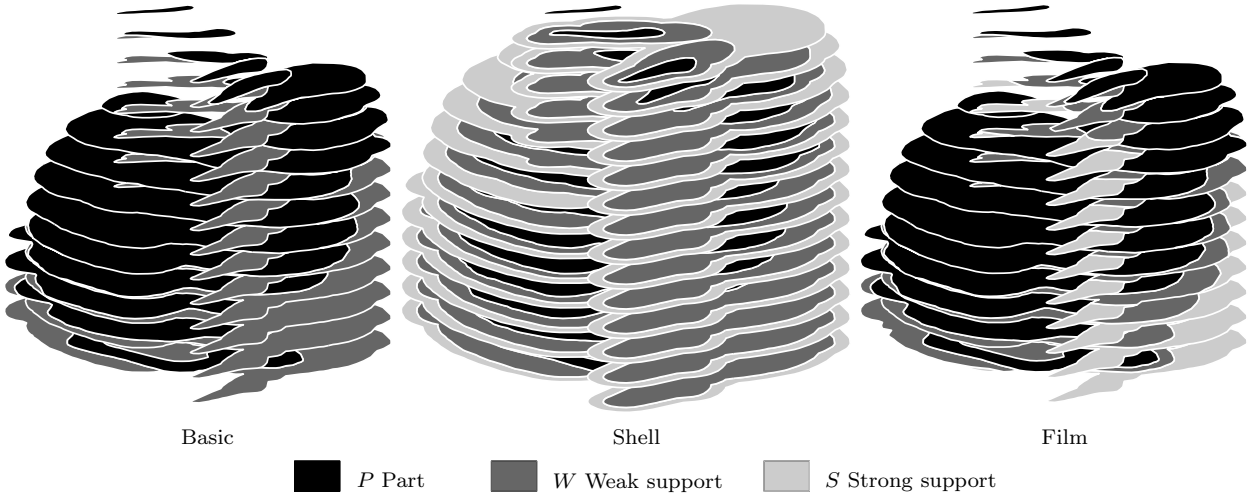


Figure 3: Support techniques applied to the Stanford bunny.

Alg. 1. The basic support technique.

```

 $M_n = P_n, \quad S_n = \emptyset, \quad i = n - 1$ 
while  $i > 0$ 
   $M_i = M_{i+1} \cup P_i, \quad S_i = M_i \setminus P_i, \quad i = i - 1$ 
end

```

shown in Alg. 1 are used to produce the corresponding support region S_i for each layer, with M_i then being a merged region for each layer, representing the union of all part regions at that layer and above. Figure 4 shows the basic method applied to the top four layers of the Stanford bunny.

2.2. Shell Technique

The shell technique, shown in Figs. 2, 3, and 5, is an adaptation of the basic technique, for *collapsible* support materials, i.e., those that remain in a soft state following deposition. Typical examples include gels and semi-solids; liquids can be used in some cases, though the buoyancy of the part material within the liquid becomes an important limiting factor in this case.

The main modification to the basic technique is the addition of a retaining shell to hold the weak support material in place. The retaining shell material must be made

with a strong material, the part material itself being the simplest choice. If the shell material *bonds* to the part material, the support generation algorithm must guarantee that they do not touch. The simplest way to accomplish this is to ensure there is always a weak support material *buffer* between the part and the shell.

The support buffer volume can be defined through 2D or 3D processing of the part geometry. A 3D technique could involve using the marching cubes algorithm [21] to produce offset surfaces from the object, thereby defining a *thickened* object volume. This algorithm could be applied directly to a PLY or STL file using the Uniform Mesh Re-sampling filter in MeshLab [22]. Chen and Wang also introduced a suitable algorithm for uniform offsetting of a polygonal model, based on layered depth-normal images [23].

Such a 3D technique could be used successfully in some cases, though it is preferable to separately control horizontal and vertical offsets, because the geometric control achieved with layer-based 3D printing is fundamentally different in the horizontal and vertical directions. The vertical offset is naturally specified as a discrete number of layers, while the horizontal offset is specified as a dimensioned distance. Therefore, a 2D technique, which oper-

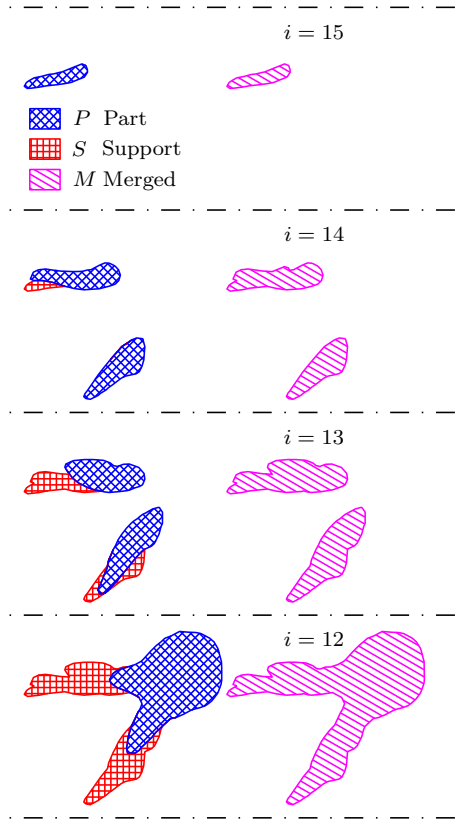


Figure 4: The basic support technique, applied to the Stanford bunny, for layers 12 to 15.

ates on the deposition layers, is preferable. Here, the basic support technique of Alg. 1 is adapted to produce the shell technique of Alg. 2.

Algorithm 2 is separated into two stages: first, the weak support regions W_i for each layer i are generated, and then the shell or strong support regions S_i are generated. Since the steps involved in creating the two types of regions are very similar, the generic function **shell** is called twice to perform these operations. For the first stage, the part regions P_i are submitted along with the horizontal and vertical support offset parameters h_W and v_W , which control the weak support thickness between the part and the shell, in the horizontal and vertical directions, respectively.

First, the array or list of layer regions B is formed, with

$$B = [\{B_1\} \{B_2\} \cdots \{B_n\}]$$

where B_i represents the union of A_i to A_n . This step is identical to Alg. 1, except that support contours are not computed at this stage. Next, B is transformed to create the vertical and horizontal buffers. The vertical buffer v layers thick is created by simply shifting B upward by v layers, with the first v layers of B simply being equated to B_1 , as shown in step 5 of the **shell** function. A horizontal buffer is created by buffering or offsetting B_i by h units outward for every layer i . Finally, C_i is found by subtracting A_i from B_i . The outputs of this process are B and

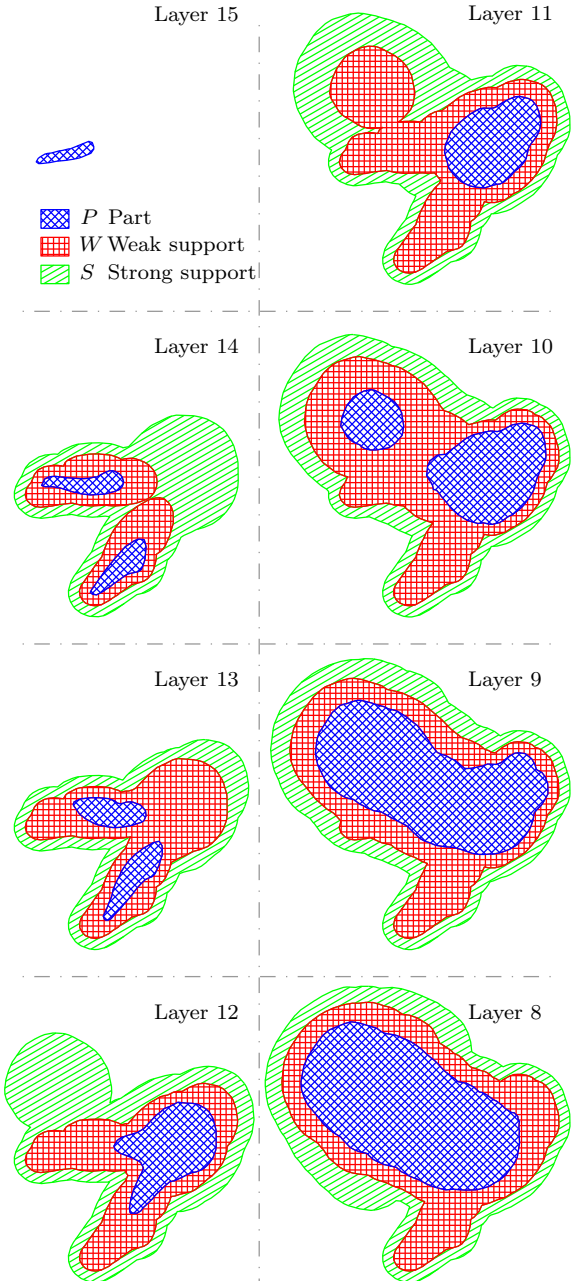


Figure 5: The shell support technique, applied to the Stanford bunny, for layers 8 to 15.

C , which are the local variables of **shell** that become the merged region array M and the weak support region array W , respectively.

As shown in Alg. 2, the **shell** function is applied a second time, with the merged region array M and the buffering parameters h_S and v_S as input, to produce the strong support region array S . Through the selection of the four parameters h_W , v_W , h_S and v_S , the shell technique allows for separate vertical and horizontal buffer control, specific to each support material.

The concept of path buffering, or offsetting, is applied frequently during this process. Path buffering trans-

Alg. 2. The shell support technique.

$$[M, W] = \mathbf{shell}(P, h_W, v_W)$$

$$[-, S] = \mathbf{shell}(M, h_S, v_S)$$

```

function [B, C] = shell(A, h, v)
1  Bn = An,   i = n,
2  while i > 0
3    Bi = Bi+1 ∪ Ai,   i = i - 1
4  end
5  B = [underbrace{{B1} ⋯ {B1}}v layers {B1} {B2} ⋯ {Bn-v}]
6  for i = 1 to n
7    Bi = buffer Bi by h outward
8    Ci = Bi \ Ai
9  end

```

forms a set of contours defining a two-dimensional region into a second set, which has been offset inward or outward by a certain distance. Path buffering is implemented here using BUFFERF [24], which is a modified version of the Matlab BUFFERM function in the Mapping Toolbox. Both BUFFERF and BUFFERM call the Mapping Toolbox function POLYBOOL to perform the needed boolean operations. POLYBOOL uses the General Polygon Clipper Library (GPC) written by Murta [25]. Following the Mapping Toolbox convention, the points of external contours are ordered clockwise and those of internal contours counterclockwise. Path coordinates are stored as NaN-delimited vectors or in cell arrays, with each cell containing the coordinates for one contour.

2.3. Film Technique

The shell technique is robust and compatible with any 3D geometry, but also wasteful and time-consuming because of the large volume of support material needed. Additionally, the weak support material must be carefully chosen, since if it is relatively inviscid or liquid, its density must be carefully matched with that of the part material to prevent buoyancy effects. Even if this material is more solid, care must be taken to ensure that the part material does not move after deposition. As seen in Fig. 3, the shell technique also uses the most material, by far, from among the three methods shown.

For this reason, the film technique is introduced, which requires the same amount of support material as the basic technique, but is not compatible with *any* part geometry. It can be used if support removal is possible, which depends on the part geometry and deposition material properties. The weak or soft support is used much less for this technique, resulting in a more rigid support structure, greatly reducing the buoyancy problem associated with the shell technique. The film technique is shown graphically in Figs. 2, 3, and 6, and algorithmically in Alg. 3. Figure 7 displays an animation comparing all three support methods, at all 15 slice layers shown in Fig. 1.

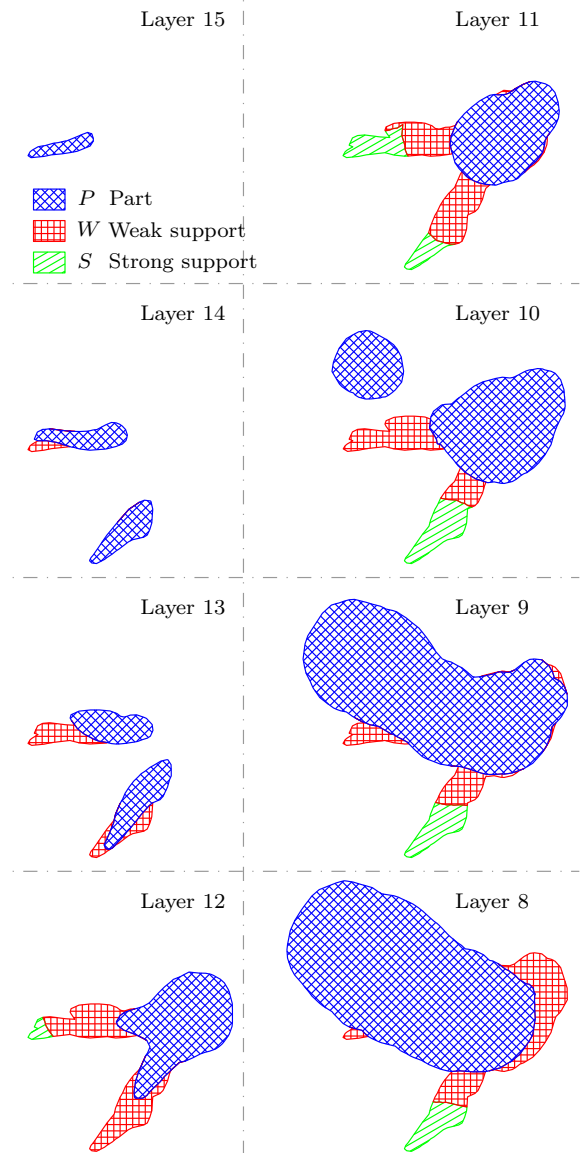
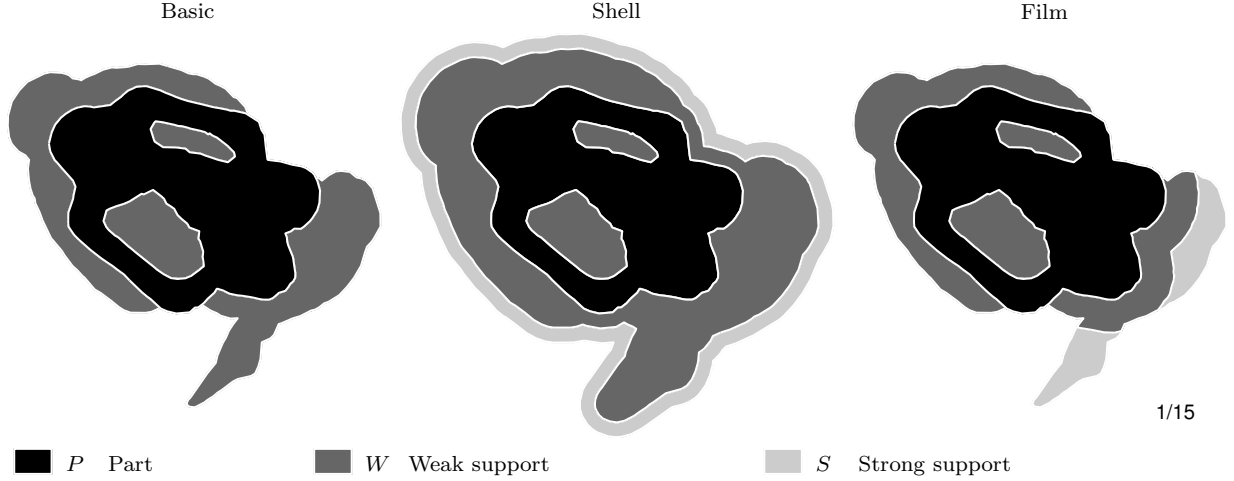


Figure 6: The film technique, applied to the Stanford bunny, for layers 8 to 15.

The film technique also requires strong and weak support materials, but the support material roles are different than for the shell technique. The technique is best understood by first assigning the strong support material to the support regions generated with the basic method. Next, a buffer zone for the soft support material is created between the part and the strong support. This zone is then subtracted from the strong support material regions.

Algorithm 3 shows how this process works mathematically, using set operations. First, the merged region array M is created as it was with the basic technique. A new region array R is also created where R_i is simply P_i buffered outward by a distance h , thereby imposing the horizontal buffering. Next, vertical buffering is accomplished by defining a new region T_i at each layer i , which represents the union of R_{i-v} to R_{i+v} . Finally, the weak or film sup-



1/15

Figure 7: Animation comparing the three support methods for the part shown in Fig. 1. To save the animation or open it in an external video player, right-click the attachment icon:

Alg. 3. The film support technique.

```

1   $M_{i+1} = \emptyset, W_n = \emptyset, i = n$ 
2  while  $i > 0$ 
3     $M_i = M_{i+1} \cup P_i$ 
4     $R_i = \text{buffer } P_i \text{ by } h \text{ outward}, i = i - 1$ 
5  end
6  for  $i = 1$  to  $n$ 
7     $j_{\min} = \max(1, i - v), j_{\max} = \min(n, i + v)$ 
8     $T_i = R_{j_{\min}}$ 
9    for  $j = j_{\min} + 1$  to  $j_{\max}$ 
10    $T_i = T_i \cup R_j$ 
11  end
12   $W_i = M_i \cap (T_i \setminus P_i), S_i = M_i \setminus T_i$ 
13 end

```

port region W_i is defined as the difference between T_i and P_i , followed by the intersection with M_i ; the strong support region S_i is the difference between M_i and T_i .

3. Case Study

In this section, the film technique is applied to create a part using the large-scale, cable-suspended 3D foam printer shown in Fig. 8 and described in [4]. This printer has a workspace of approximately one cubic metre. The part material is polyurethane foam, the weak support is shaving foam, and the strong support is also polyurethane foam. The deposition path widths and heights are 12 mm and 10 mm, respectively, for both materials. Part errors are measured and corrected using a version of the geometric feedback algorithm described in [16]. Without this algorithm, foam deposition control is completely lost after about 20 layers.

Three parts are constructed to demonstrate the proposed support techniques: the Stanford Bunny is built

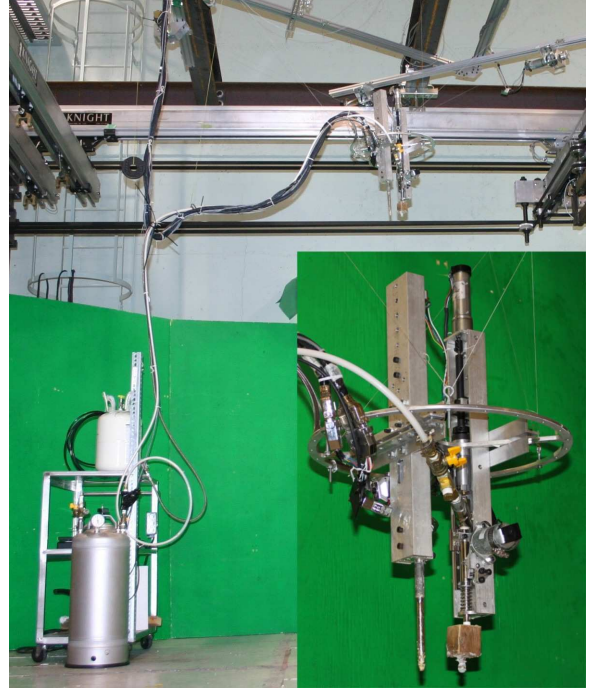


Figure 8: The cable-suspended 3D foam printer.

using the shell technique, while the film technique is used to build two interlocking chain links, and a Voronoi sphere containing a trapped solid sphere. The vertical and horizontal buffering parameters used for the shell technique in Alg. 2 are $v_w = v_s = 1$ layer and $h_w = h_s = 24$ mm, twice the deposition path width. These values are chosen mainly to minimize the necessary support material volume, with v_w and v_s being the minimum allowed values. Larger values are used for h_w to facilitate support removal and for h_s to avoid leaks of the weak support material through the strong support material shell.

For the film technique, the values selected for v and h affect the ratio of weak support to strong support material used but do not affect the total support material used. As such, these values are chosen primarily based on the strength of the weak support material: the weaker this material is, the smaller these values should be, such that the strong support material can provide more support rigidity. Since the shaving foam support material used for the 3D foam printer is particularly weak, the minimum allowed values of $v = 1$ layer and $h = 12$ mm, one deposition path width, are used.

Material regions for all 46 construction layers of the Stanford Bunny, using the shell technique, are shown in the animation of Fig. 9; photos taken during the construction process are shown in Fig. 10. Based on observations of material performance during the construction of this part, a single layer and a single path width of weak support material, i.e., $v_w = 1$ layer and $h_w = 12$ mm, would have sufficed, thereby resulting in some material savings. Additionally, it can be seen in Fig. 10 that vertical containment of the weak support material is lost in a few locations. While this is not a major problem for the Stanford bunny when built the scale shown, it would be problematic for taller parts, where the hydrostatic pressure force caused by the weak support material could potentially cause major leaks through gaps in the shell. Two layers of shell in the vertical direction would likely correct this problem, i.e. $v_s = 2$ layers and $h_w = 24$ mm would be more optimal values. Figure 11 summarizes the construction of the Stanford bunny, including timelapse photography of both the 3D printing and support removal. It should be noted that the shell technique was used for this part *only* because the film technique had not yet been developed. Clearly, this part could easily be built using the film technique, with considerable construction-time and material savings.

The film technique is first demonstrated by printing two interlocking chain links, with Fig. 12 displaying an animation of material regions for all part-construction layers and Fig. 13 showing a rendering of the CAD model and pictures of the part following construction and after support removal. Although this is a relatively simple part, it might be expected for the support removal to be difficult if the film technique is used. However, after making a few small cuts in the strong support, it is easily removed, with the entire post-processing work requiring less than five minutes.

To further establish the applicability of the film technique, a Voronoi sphere, containing a trapped solid sphere, rendered in Fig. 14, is also constructed. The PLY file for this part was produced by following a procedure available on the MeshLab blog website [26]. It was scaled to have a diameter of approximately 400 mm, resulting in 41 printed layers, which are shown in the animation of Fig. 15. Figure 16 shows a video, which summarizes the construction of the sphere, including timelapse photography of both the 3D printing and support removal.

In the lower left corner of Fig. 14, the material regions

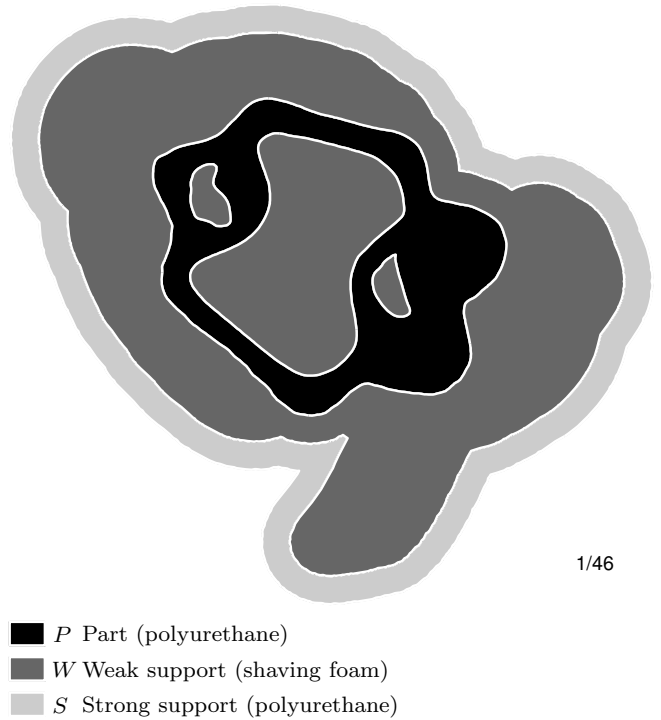


Figure 9: Animation showing the Stanford bunny material regions, using the shell technique. To save the animation or open it in an external video player, right-click the attachment icon:

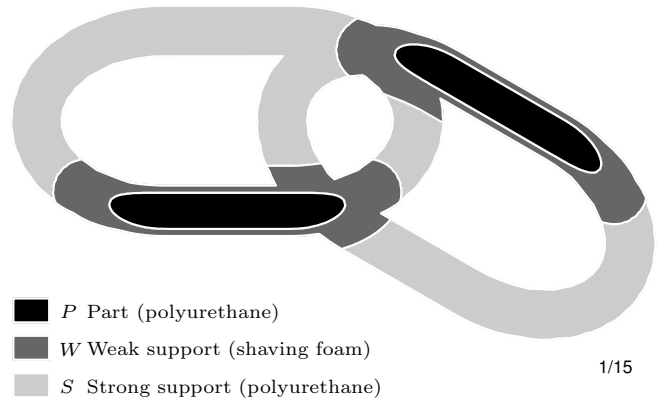


Figure 12: Animation showing the chain links material regions, using the film technique. To save the animation or open it in an external video player, right-click the attachment icon:

for the part, the weak support, and the support support are shown for layers 1–30 of 41. This diagram reveals an immediate potential problem related to support removal: the strong support intertwines through the holes of the Voronoi sphere. Even though the strong support does not touch the part, the two structures are *interlocked*. Fortunately, polyurethane foam is a relatively weak material that can be cut easily and even torn apart by hand. Therefore, despite the interlock problem, the strong support removal is straightforward. The other images of Fig. 14 show



Figure 10: The Stanford bunny, constructed using the shell technique, according to the material regions shown in Fig. 9: (left) The part and support material, after 3D printing is complete; (center) After the polyurethane retaining shell is removed; (right) The final part, after support removal.



Figure 11: Video summarizing the construction of the Stanford bunny. To save the video or open it in an external player, right-click the attachment icon:

the sphere at various stages of construction, and then after all of the support has been removed. Printing required about seven hours, polyurethane foam support removal about one hour, and shaving foam support was removed in a few minutes by spraying the part with water.

In Fig. 17, the deposition areas of layer 15 of the Voronoi sphere are shown, along with a traditional fill path technique and a different technique the authors call open fill. Much as the slice regions introduced in the previous section approximate 3D geometry, the fill paths are a 1D approximation of the 2D slice regions. In a traditional fill technique, the outer boundaries defining a material region

are offset by one half the path width to define boundary paths for a layer. Fill paths are then generated using methods such as the zig-zag or concentric contour techniques [24, 27, 28]. This type of approximation works well in general, but results in considerable error when approximating small regions or long, thin regions. This effect can be seen in the traditional fill path technique of Fig. 17, where the weak support paths are nearly overlapping in many places, and in general, they poorly approximate the corresponding weak support regions.

The open fill path technique works by initially buffering the part-region contours *outward* by one half the path

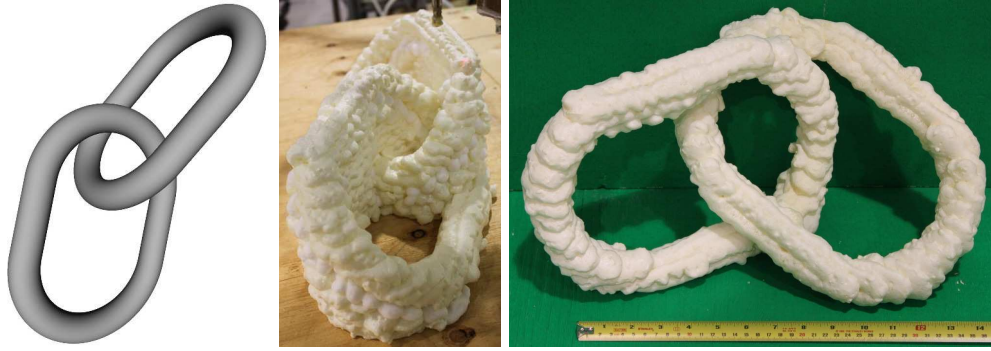


Figure 13: Two interlocking chain links, constructed using the film technique, according to the material regions shown in Fig. 12: (left) PLY file rendering; (center) The part and support material, after 3D printing is complete; (right) The final part, after support removal.

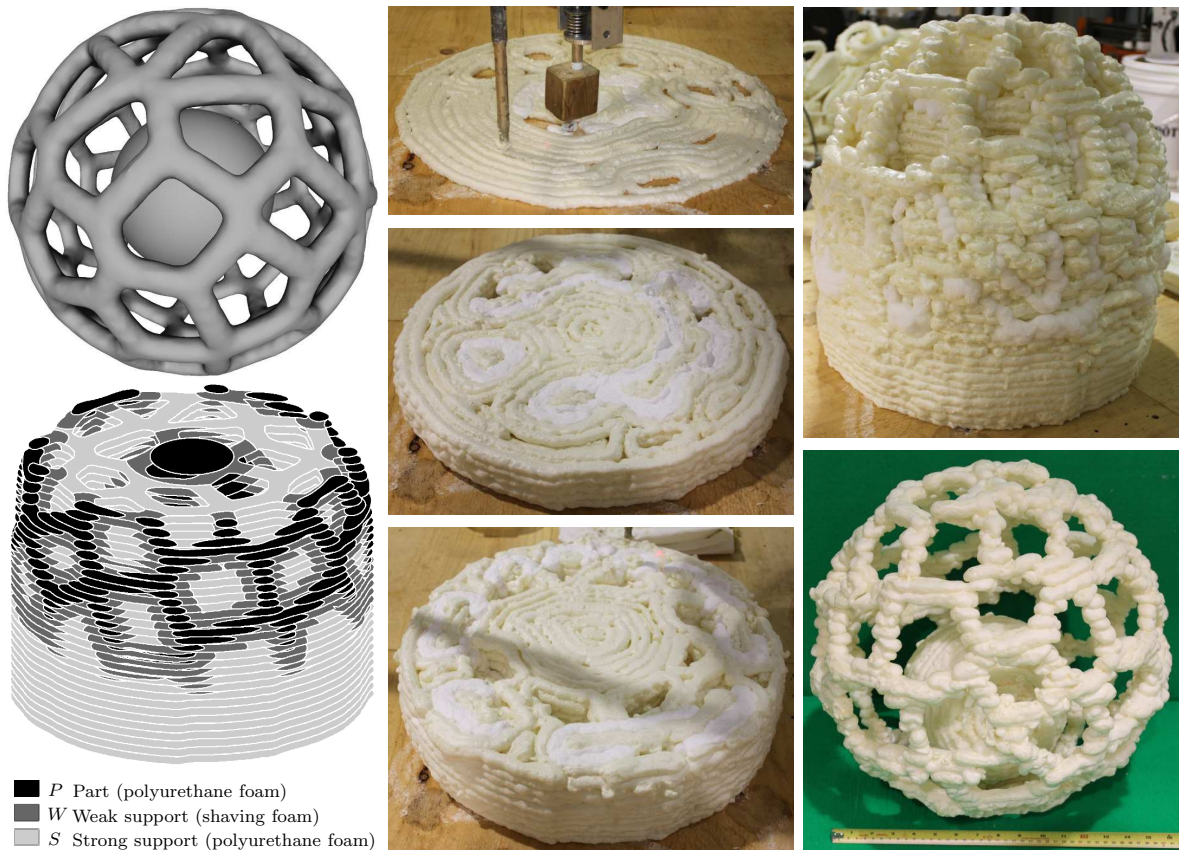


Figure 14: Voronoi sphere: (left) CAD model rendering and deposition layers 1–30 of 40, using the film support technique; (right) Images taken during construction of the 400-mm-diameter sphere.

width. Then, the sections of these contours that lie *inside* the weak support regions are designated as weak support deposition paths. Since most of the resulting paths are trimmed and do not form a closed loop, they are called open fill paths. Next, the support regions are trimmed to accommodate the open fill paths and these reduced regions are filled using the traditional concentric-contour fill method. As seen in Fig. 17, this procedure results in a much better approximation of the weak support regions.

Moreover, it should be noted that the primary purpose of the support material paths is to *support* the part ma-

terial paths, and not simply to provide the best approximation of the support material regions. It might seem that these two purposes are best satisfied with the same support path geometry, but this is not the case. If the weak support paths for the traditional method of Fig. 17 are again considered, the nearly overlapping weak support paths near the part paths will cause too much material to be deposited, pushing against the part and destroying some of the part geometry. The open fill path method, by contrast, moves the overlapping weak support paths away from the part regions, where they will minimally affect the

Figure 16: Video summarizing the construction of the Voronoi sphere.

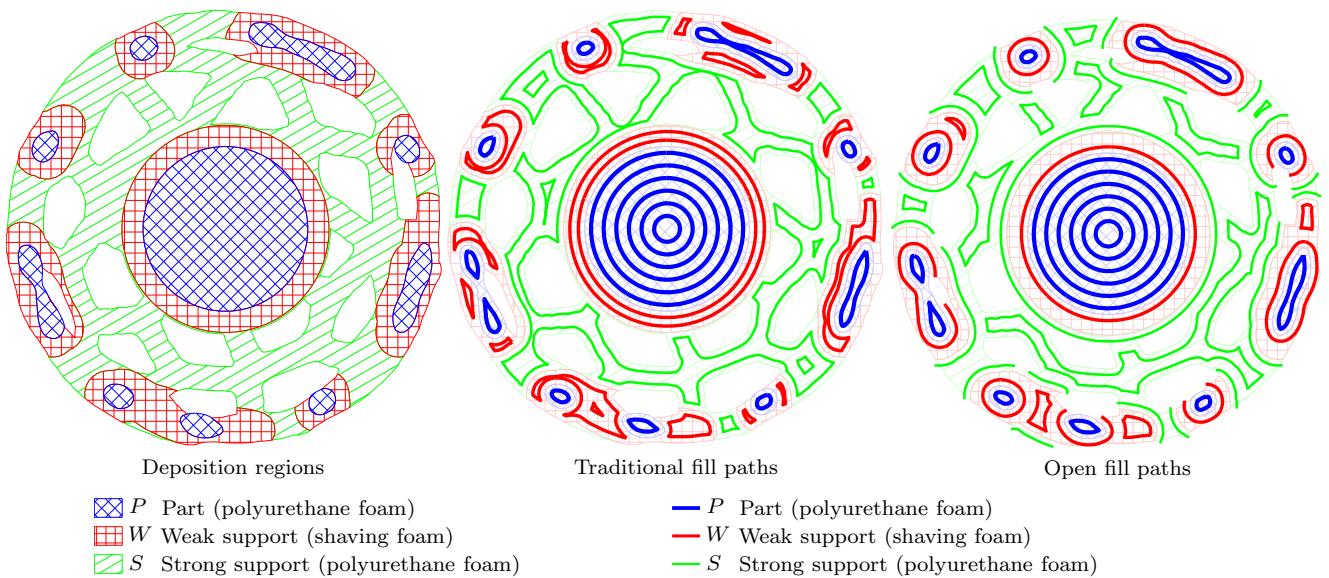


Figure 17: Fill techniques for layer 15 of the Voronoi sphere. The sphere diameter is 400 mm and the path width is 12 mm.

part accuracy.

4. Discussion

The 3D printer introduced in the Case Study uses polyurethane foam and shaving foam as demonstration materials for large-scale additive manufacturing. This printer is part of a larger research project, which involves the devel-

opment of automated robot-driven fabrication technology capable of producing large-scale architectural prototypes. As such, it is expected that the shell and film techniques can be adapted for use with earth-based construction materials such as concrete.

The main advantage of the two techniques is their potential for use with AM materials that can be deposited in a semi-solid state but require a significant amount of time



- *P* Part (polyurethane)
- *W* Weak support (shaving foam)
- *S* Strong support (polyurethane)

Figure 15: Animation showing the Voronoi sphere material regions, using the film technique. To save the animation or open it in an external video player, right-click the attachment icon:

to harden or cure sufficiently to support their own weight. Candidate materials should satisfy a few basic characteristics. Firstly, they should be storable in the printable state for a minimum of a few hours, but preferably indefinitely. Precise deposition control should be possible using an extrusion-based or pressurized-tank system. After deposition, materials should cure or harden to their final state within a few minutes. Additionally, the strong support material must be rigid enough to support its own weight. The weak support material must be easy to remove, must not degrade the part, and should not be so weak that buoyancy effects become significant and deposited part material *moves* following deposition.

A second significant advantage of these two techniques is the potential for rapid support removal following construction. For example, the strong support used to construct the Voronoi sphere is easily broken apart by hand and removed, even though it is interlocked with the part. Although this approach is clearly unsuitable for many materials, the film support technique could be adapted to include cracks in the strong support material, filled with the weak material and strategically placed to facilitate support removal.

For many AM techniques, support removal is a major manual component of an otherwise automated construction process, adding significantly to production time and cost. For example, for FDM using polycarbonate

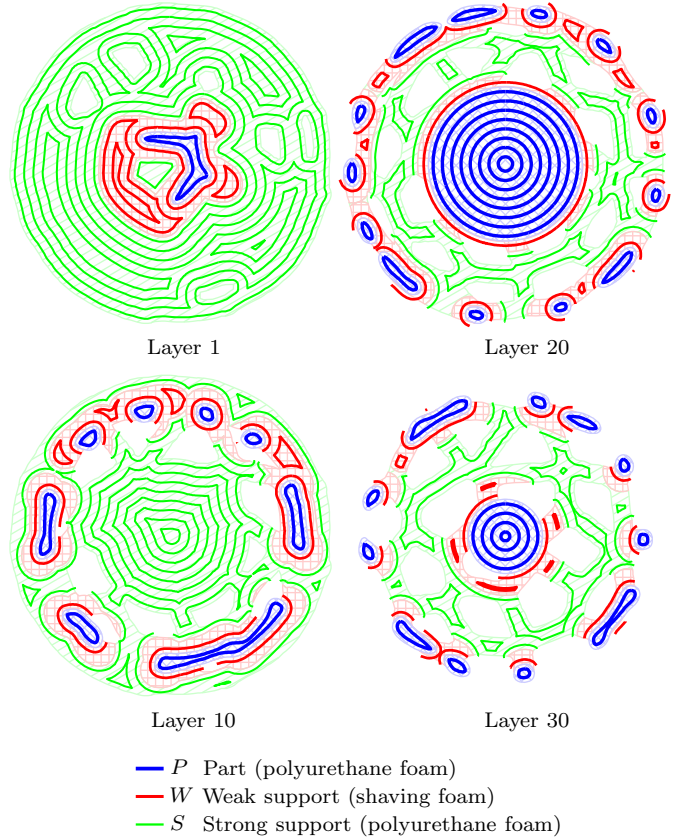


Figure 18: Open fill path method for four layers of the Voronoi sphere. The sphere diameter is 400 mm and the path width is 12 mm.

(PC), supports are broken away following part construction, which can be time-consuming, damaging to the part, and significantly restricts the printable geometry because most internal cavities cannot be printed [29, p. 164]. The film technique could be used to address all of these issues. Even internal cavities could be printed, since artificial cracks could be added to internal support volumes to divide them into pieces small enough to be extracted through holes.

The computational burden for algorithms 1–3 is relatively low, particularly when compared to the cost of the path buffering used to transform the two-dimensional regions into one-dimensional paths. For the Stanford bunny part, computational times were 0.5 s, 1.9 s, and 1.9 s, respectively, for the basic, shell, and film techniques. For the Voronoi sphere, the required time was 26.3 s, using the film technique. Path buffering needed to create the fill paths for all 40 layers of the Voronoi sphere required 73.4 s for the traditional fill paths and 131.6 s for the open fill paths. All computations were performed in Matlab r2011b using an Intel Core i7-2720QM processor (Quad-core, 2.2 GHz, 3.3 GHz turbo). Computations that do not involve multiple layers were distributed *at the layer level* across all four processor cores using **parfor** loops in MATLAB. The most computationally expensive operation, by far, is the path

buffering, which never involves computations on data from multiple layers, and can therefore always be parallelized at the layer level.

The open fill path method introduced in Section 3 clearly lowers the error associated with approximating the two-dimensional material regions, compared to the traditional method, which uses closed paths only. However, open paths are currently used only for the support at the material interfaces; closed paths are used at all other locations.

Extending the application of the open fill path method would lead to even better approximation of the two-dimensional material regions. For example, closed paths often result in significant approximation error when path buffering is performed near the center of a fill region, where nearly overlapping paths can result in one extreme, and material voids in the other. When a path contains sections that are separated by slightly more than $2d$, buffering that path inward by a distance d will produce a new path with sections that are nearly overlapping. Conversely, when a polygon contains sections that are separated by slightly less than $2d$, the corresponding sections of the buffered polygon will be deleted. If open fill paths were applied in these cases, both of these path sections would be replaced by a single open path, resulting in a much better approximation of the geometry. For example, the central weak support region of Layer 30 in Fig. 18 contains seven weak support paths, two of which are open and five of which are closed. Clearly, the approximation of this region would be much more accurate if *all* seven paths were open.

5. Conclusions

Two novel support techniques were introduced, which are particularly suitable for AM processes that involve weak support materials. The shell technique was shown to be applicable for constructing any 3D geometry, though also inefficient in terms of material use. Therefore, the film technique was also introduced, which is less versatile but requires much less support material. Both techniques were demonstrated by constructing objects with an experimental large-scale 3D foam printer. A method for adapting the film technique for harder support materials was discussed, and the computational performance of both techniques were compared to the basic support technique. A broad description was also provided for a new open fill path technique, along with a framework for generalizing the technique to increase the accuracy of planar region approximation with one-dimensional paths. The techniques developed in this paper are believed to contribute significantly to providing designers with as much freedom as possible by ensuring efficient and versatile 3D printing capabilities for a broad variety of materials.

Acknowledgments

The authors gratefully acknowledge the support of The Social Sciences and Humanities Research Council of Canada (SSHRC), under Strategic Research Grant 890-2011-0039, led by Prof. Aaron Sprecher, McGill University. This work was also supported by the Le Fonds de Recherche du Québec –Nature et Technologies (FRQ-NT), in the form of a postdoctoral fellowship for E. Barnett.

References

- [1] R. A. Buswell, R. C. Soar, A. G. F. Gibb, A. Thorpe, Freeform construction: Mega-scale rapid manufacturing for construction, *Automation in Construction* 16 (2007) 224–231.
- [2] B. Khoshnevis, Automated construction by contour crafting—related robotics and information technologies, *Automation in Construction* 13 (2004) 5–19.
- [3] E. Dini, Method for automatically producing a conglomerate structure and apparatus therefor, US Patent 8,337,736 (2012).
- [4] E. Barnett, C. Gosselin, Large-scale 3D printing with a cable-suspended robot, *Additive Manufacturing* (2015) accepted.
- [5] C. R. Deckard, Method and apparatus for producing parts by selective sintering, US Patent 4,863,538 (Sep. 5 1989).
- [6] C. W. Hull, Apparatus for production of three-dimensional objects by stereolithography, US Patent 4,575,330 (Mar. 11 1986).
- [7] S. S. Crump, Apparatus and method for creating three-dimensional objects, US Patent 5,121,329 (Jun. 9 1992).
- [8] K. Chalasani, L. Jones, L. Roscoe, Support generation for fused deposition modeling, in: *Solid Freeform Fabrication Symposium*, Austin, TX, 1995, pp. 229–241.
- [9] X. Huang, C. Ye, J. Mo, H. Liu, Slice data based support generation algorithm for fused deposition modeling, *Tsinghua Science & Technology* 14 (S1) (2009) 223–228.
- [10] D. E. Snead, D. R. Smalley, A. L. Cohen, J. W. Allison, T. J. Vorgitch, T. P. Chen, Boolean layer comparison slice, US Patent 5,854,748 (Dec. 29 1998).
- [11] T. A. Kerekes, J. M. Earl, P. H. Marygold, C. R. Manners, J. S. Thayer, Method and apparatus for data manipulation and system control in a selective deposition modeling system, CA Patent 2,233,202 (Apr. 3 1997).
- [12] W. Wang, T. Y. Wang, Z. Yang, L. Liu, X. Tong, W. Tong, J. Deng, F. Chen, X. Liu, Cost-effective printing of 3D objects with skin-frame structures, *ACM Trans. Graph.* 32 (6) (2013) 177:1–177:10.
- [13] J. Vanek, J. A. G. Galicia, B. Benes, Clever support: Efficient support structure generation for digital fabrication, *Computer Graphics Forum* 33 (5) (2014) 117–125.
- [14] J. Dumas, J. Hergel, S. Lefebvre, Bridging the Gap: Automated steady scaffolds for 3D printing, *ACM Trans. Graph.* 33 (4) (2014) 98:1–98:10.
- [15] E. Barnett, J. Angeles, D. Pasini, P. Sijpkens, Robot-assisted rapid prototyping for ice structures, in: *IEEE Int. Conf. Robot. Autom.*, Kobe, JP, May 12–17, 2009, pp. 146–151.
- [16] E. Barnett, J. Angeles, D. Pasini, P. Sijpkens, Surface Mapping Feedback for robot-assisted rapid prototyping, in: *Proc. IEEE Int. Conf. Robot. Autom.*, Shanghai, China, 2011, pp. 3739–3744.
- [17] L. M. B. Rodgers, Extrusion-based additive manufacturing process with part annealing, US Patent 13/081,956 (Oct. 11 2012).
- [18] S. S. Crump, J. W. Comb, W. R. Priedeman, R. L. Zinniel, Process of support removal for fused deposition modeling, US Patent 5,503,785 (Apr. 2 1996).
- [19] E. Kritchman, H. Gothait, G. Miller, System and method for printing and supporting three dimensional objects, US Patent 7,364,686 (Apr. 29 2008).

- [20] Stanford Computer Graphics Laboratory, The Stanford 3D Scanning Repository, <http://graphics.stanford.edu/data/3Dscanrep/> (2014).
- [21] W. E. Lorensen, H. E. Cline, Marching cubes: A high resolution 3D surface construction algorithm, *SIGGRAPH Comput. Graph.* 21 (4) (1987) 163–169.
- [22] P. Cignoni, MeshLab, Visual Computing Lab ISTI-CNR, <http://meshlab.sourceforge.net/> (2014).
- [23] Y. Chen, C. C. L. Wang, Uniform offsetting of polygonal model based on layered depth-normal images, *Computer-Aided Design* 43 (1) (2011) 31–46.
- [24] E. Barnett, J. Angeles, D. Pasini, P. Sijpkens, A heuristic algorithm for slicing in the rapid freeze prototyping of sculptured bodies, in: J. Angeles, B. Boulet, J. J. Clark, J. Kovacs, K. Siddiqi (Eds.), *Brain, Body, and Machine*, Springer-Verlag, Berlin, 2010, pp. 149–162.
- [25] A. Murta, GPC general polygon clipper library, <http://www.cs.man.ac.uk/~toby/gpc/> (2014).
- [26] The MeshLab Blog, Creating Voronoi sphere, <http://meshlabstuff.blogspot.ca/2009/03/creating-voronoi-sphere.html> (2009).
- [27] R. T. Farouki, T. Koenig, K. A. Tarabanis, J. U. Korein, J. S. Batchelder, Path planning with offset curves for layered fabrication processes, *Journal of Manufacturing Systems* 14 (5) (1995) 355–368.
- [28] Y. Jin, Y. He, J. Fu, W. Gan, Z. Lin, Optimization of tool-path generation for material extrusion-based additive manufacturing technology, *Additive Manufacturing* 1–4 (2014) 32–47, Inaugural Issue.
- [29] I. Gibson, D. Rosen, B. Stucker, *Additive Manufacturing Technologies: Rapid Prototyping to Direct Digital Manufacturing*, Springer US, 2009.